• Basic Research •

Amyloid-β-induced pyroptosis drives retinal neurodegeneration in a TgAPPswePS1 mouse model

Jia-Rong Cao[1], Juan Li[2], Hai-Hua Zheng[1], Zhi-Zhang Dong[1]

[1]Department of Ophthalmology, the Second Affiliated Hospital and Yuying Children's Hospital of Wenzhou Medical University, Wenzhou 325000, Zhejiang Province, China
[2]Department of Ophthalmology, Xi'an People's Hospital (Xi'an Fourth Hospital), Xi'an 710004, Shaanxi Province, China

Correspondence to: Zhi-Zhang Dong and Hai-Hua Zheng. Department of Ophthalmology, the Second Affiliated Hospital and Yuying Children's Hospital of Wenzhou Medical University, No.109, Xueyuanxi Road, Wenzhou 325000, Zhejiang Province, China. dongzhizhang@wzhealth.com; eyezhh@126.com

Received: 2025-06-18 Accepted: 2025-07-24

Abstract

• **AIM:** To investigate whether pyroptosis contributes to retinal ganglion cell (RGC) degeneration in aged TgAPPswePS1 transgenic mice and to explore the relationship between amyloid-beta (Aβ) accumulation and activation of the pyroptotic pathway in the retina.

• **METHODS:** The twelve 18-month-old TgAPPswePS1 transgenic mice and twelve 18-month-old wild-type C57BL/6J mice were used to investigate amyloid precursor protein (APP) and Aβ expression, retinal structural changes, and activation of pyroptosis in RGCs. Immunohistochemical analyses were performed to detect APP, Aβ, and pyroptosis-related proteins [NOD-like receptor thermal protein domain associated protein 3 (NLRP3), caspase-1, gasdermin D (GSDMD), interleukin (IL)-1β, and IL-18]. Quantitative assessments of retinal nerve fiber layer (RNFL) thickness were conducted to evaluate retinal integrity.

• **RESULTS:** Compared to age-matched wild-type controls, TgAPPswePS1 transgenic mice exhibited significant upregulation of APP and Aβ within RGCs. Histological analysis revealed reduced RNFL thickness, indicating structural degeneration. Notably, RGCs in transgenic mice showed robust immunoreactivity for NLRP3, caspase-1, and GSDMD, alongside elevated levels of IL-1β and IL-18, supporting the activation of pyroptosis.

• **CONCLUSION:** Aβ accumulation in RGCs is associated with retinal degeneration and activation of the pyroptosis pathway in aged TgAPPswePS1 mice. This study provides new insights into the inflammatory mechanisms underlying Aβ-related retinal neurodegeneration and suggests that targeting pyroptosis may represent a promising therapeutic strategy for retinal disorders linked to amyloid pathology.

• **KEYWORDS:** retinal ganglion cell; amyloid-beta; pyroptosis; TgAPPswePS1; NLRP3 inflammasome

DOI:10.18240/ijo.2025.11.03

Citation: Cao JR, Li J, Zheng HH, Dong ZZ. Amyloid-β-induced pyroptosis drives retinal neurodegeneration in a TgAPPswePS1 mouse model. *Int J Ophthalmol* 2025;18(11):2031-2036

INTRODUCTION

The progressive loss of retinal ganglion cells (RGC) is a hallmark of numerous retinal neurodegenerative disorders, including glaucoma, diabetic retinopathy, and age-related macular degeneration, ultimately leading to irreversible vision impairment and blindness[1]. Despite advances in understanding the pathophysiology of these conditions, the exact molecular and cellular mechanisms underlying RGCs degeneration remain elusive, posing a major barrier to the development of effective neuroprotective strategies.

Among the various pathological factors implicated in neuronal loss, amyloid-beta (Aβ), a neurotoxic peptide derived from the cleavage of amyloid precursor protein (APP), has garnered significant attention[2-3]. Aβ accumulation is widely recognized as a key contributor to synaptic dysfunction and neuronal death in Alzheimer's disease (AD), and increasing evidence suggests that similar pathogenic mechanisms may also operate in the retina, often described as a "window to the brain"[4]. Aβ deposition has been observed in the retina of patients with AD and in transgenic animal models, where it correlates with progressive RGCs damage and visual deficits[5]. While apoptosis has traditionally been considered the dominant mechanism of Aβ-induced neurotoxicity in RGCs, growing research indicates that alternative modes of programmed cell death may also be involved[6].

Pyroptosis, a form of programmed cell death distinct from apoptosis and necrosis, has recently emerged as a critical mediator of inflammation-driven neurodegeneration[7].

Unlike apoptosis, pyroptosis is characterized by cell swelling, membrane rupture, and the release of pro-inflammatory intracellular contents[8]. This process is orchestrated through the activation of the NOD-like receptor thermal protein domain associated protein 3 (NLRP3) inflammasome, which recruits and activates caspase-1, leading to the cleavage of gasdermin D (GSDMD) and the maturation and release of interleukin (IL)-1β and IL-18[9-10]. Pyroptosis plays a pivotal role in amplifying neuroinflammation and tissue damage, and its involvement has been increasingly recognized in both central nervous system diseases and ocular disorders[11]. However, the role of pyroptosis in Aβ-mediated RGCs death remains largely unexplored.

Given the retina's vulnerability to both Aβ toxicity and chronic inflammation, elucidating the contribution of pyroptosis to RGCs degeneration in the context of Aβ accumulation is of considerable importance. In this study, we employed aged TgAPPswePS1 transgenic mice, a well-established model of Aβ overproduction[12], to investigate the involvement of pyroptotic pathways in RGCs death. We aimed to assess the extent of Aβ deposition and the activation of pyroptosis-related molecules, thereby providing novel mechanistic insights into the interplay between neuroinflammation and retinal neurodegeneration. Understanding these processes may help identify new therapeutic targets for preventing or slowing vision loss in retinal degenerative diseases.

MATERIALS AND METHODS

Ethical Approval All animal procedures were conducted in strict accordance with the Guide for the Care and Use of Laboratory Animals (Institute of Laboratory Animal Resources) and the Public Health Service Policy on Humane Care and Use of Laboratory Animals. Experimental protocols were approved by the Second Affiliated Hospital and Yuying Children's Hospital of Wenzhou Medical University (No. xmsq2023_0837).

Animal Models Mice were housed in a controlled environment under white fluorescent lighting at an intensity of approximately 200 lx, with a 12-hour light/dark cycle. Standard rodent chow and water were provided *ad libitum*. The following mouse strains were used: 12 18-month-old APPswe/PS1ΔE9 (APP/PS1) double-transgenic mice (6 males and 6 females) obtained from The Jackson Laboratory (Bar Harbor, ME, USA) and 12 wild-type C57BL/6J mice (6 males and 6 females) of the same background and age. Both male and female animals, aged to reflect late-stage amyloid pathology, were included in the experiments.

Histology of Retinal Cross-Sections All mice were euthanized by intraperitoneal injection of sodium pentobarbital (150 mg/kg). The eyeballs were carefully enucleated and the dorsal side was marked for orientation after euthanasia. The eyeballs were fixed in 4% glutaraldehyde for initial cross-linking, followed by immersion in 4% paraformaldehyde for further fixation. Samples were then embedded in methacrylate resin and sectioned along the dorsal-ventral axis at a thickness of 1 μm. Retinal sections were stained with hematoxylin and eosin (H&E) to evaluate overall retinal morphology. High-resolution images were captured at 20× and 40× magnifications using a light microscope[13].

Immunohistochemistry Paraffin-embedded retinal sections were mounted on poly-L-lysine-coated glass slides and processed using an automated immunostaining system (Ventana BenchMark XT; Ventana Medical Systems, Tucson, AZ, USA) according to the manufacturer's protocol[14]. Antigen retrieval was performed as per standard protocol. Sections were incubated with the following primary antibodies: mouse anti-APP (1:100, #RHC12509, Chemicon, MA, USA), and mouse anti-Aβ (1:100, #803001, Covance, PA, USA). Visualization was achieved using the appropriate detection kits, and all slides were counterstained with Mayer's hematoxylin to highlight nuclear morphology. Semi-quantitative analysis in RGCs using Image-Pro Plus version 6.0 (Media Cybernetics, Silver Spring, CA, USA).

Immunofluorescence Staining For immunofluorescence analysis[15], eyes were enucleated, fixed in 4% paraformaldehyde for 30min, and cryo-protected using a graded sucrose series (10%, 20%, and 30%). Tissues were embedded in optimal cutting temperature compound and sectioned at 10 μm thickness using a cryostat. Sections were blocked and permeabilized before incubation with the following primary antibodies: rabbit anti-NLRP3 (1:500, #15101, Cell Signaling Technology, MA, USA), rabbit anti-caspase-1 (1:800, #24232, Cell Signaling Technology, MA, USA), rabbit anti-GSDMD (1:500, #69469, Cell Signaling Technology, MA, USA), rabbit anti-IL-1β (1:400, #20021, Proteintech, Wuhan, China), and rabbit anti-IL-18 (1:300, #20324, Mlbio, Shanghai, China).

Secondary antibodies conjugated with Alexa Fluor 488 or 594 fluorophores (Thermo Fisher Scientific, Waltham, MA, USA) were applied at a dilution of 1:1000. Nuclear counterstaining was performed using 4',6-diamidino-2-phenylindole (DAPI, #21490, Thermo Fisher Scientific, MA, USA). Images were acquired using a Zeiss LSM 700 confocal microscope (Carl Zeiss Meditec, Dublin, CA, USA), and identical imaging settings were applied across groups to ensure comparability. Semi-quantitative analysis in RGCs using Image-Pro Plus version 6.0 (Media Cybernetics, Silver Spring, CA, USA).

Statistical Analysis Data were analyzed and visualized using GraphPad Prism version 7.0 (GraphPad Software, La Jolla, CA, USA). All values are presented as mean±standard error of the mean (SEM) from a minimum of three independent biological replicates. Group comparisons were conducted

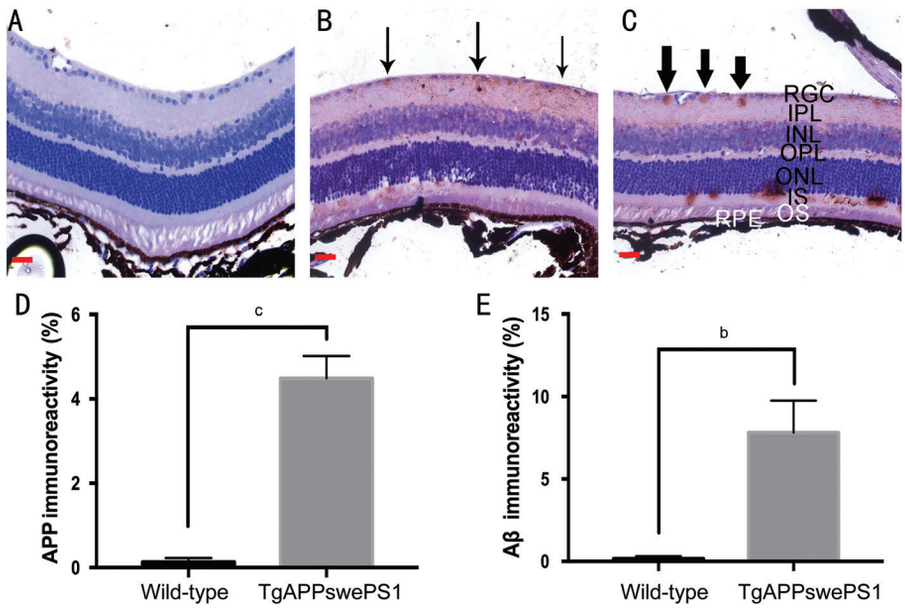

Figure 1 Immunohistochemical analysis of retinal sections from wild-type and TgAPPswePS1 transgenic mice (scale bar=50 μm) A: Retinal structure of a wild-type mouse showing normal morphology; B: APP immunoreactivity in the RGC layer of a TgAPPswePS1 mouse, with APP deposition indicated by a thin arrow; C: Aβ immunoreactivity in the RGC layer of a TgAPPswePS1 mouse, with Aβ deposition indicated by a thick arrow; D–E: Semi-quantitative analysis of immunohistochemical intensity reveals significant upregulation of APP and Aβ in TgAPPswePS1 mice compared to wild-type controls. $^{b}P<0.01$, $^{c}P<0.001$. RNFL: Retinal nerve fiber layer; RGC: Retinal ganglion cell layer; IPL: Inner plexiform layer; INL: Inner nuclear layer; OPL: Outer plexiform layer; ONL: Outer nuclear layer; IS: Inner segment; OS: Outer segment; RPE: Retinal pigment epithelium; APP: Amyloid precursor protein; Aβ: Amyloid-beta.

using the non-parametric Mann-Whitney *U* test. A *P*-value less than 0.05 was considered statistically significant.

RESULTS

APP and Aβ Expression in RGCs of Aged TgAPPswePS1 Transgenic Mice Aβ, a peptide of 39–43 amino acids, is produced through sequential proteolytic cleavage of APP[16]. To assess APP expression in RGCs, we performed immunostaining using an APP-specific antibody. In control (wild-type) mice, APP immunoreactivity was negligible within the RGC layer. In contrast, aged TgAPPswePS1 transgenic mice demonstrated robust APP expression in RGCs, as indicated by distinct brownish-yellow staining. Quantitative analysis revealed a 4.485±0.529-fold increase in APP expression in transgenic mice compared to controls ($P<0.01$), indicating substantial upregulation of APP in RGCs of TgAPPswePS1 mice. To determine the extent of Aβ accumulation, retinal sections were subjected to immunohistochemical staining using an Aβ-specific antibody. Control retinas exhibited minimal Aβ immunoreactivity, with only background staining detected. In contrast, strong Aβ staining was observed in RGCs of TgAPPswePS1 mice. Quantification revealed a 7.815±0.145-fold increase in Aβ levels in the transgenic group compared to controls ($P<0.01$), confirming pronounced Aβ deposition in the RGC layer (Figure 1).

Retinal Structural Alterations in Aged TgAPPswePS1 Transgenic Mice To evaluate structural integrity of the retina, histological examination was conducted on retinal cross-sections. Qualitative analysis showed that overall retinal architecture was preserved in TgAPPswePS1 mice, with no overt signs of disorganization or laminar disruption. The RNFL, ganglion cell layer (GCL), inner and outer nuclear layers (INL and ONL), and plexiform layers (IPL and OPL) all retained their stratified structure, comparable to control retinas (Figure 2A–2B).

However, quantitative analysis revealed significant thinning of the RNFL in TgAPPswePS1 mice (15.33±0.67 μm) compared to controls (22.00±1.16 μm, $P=0.0075$), indicating early neurodegenerative changes (Figure 2C).

Increased Expression of Pyroptosis-Related Proteins in RGCs of Aged TgAPPswePS1 Mice To investigate whether pyroptosis contributes to RGC degeneration, we examined the expression of key pyroptotic markers. NLRP3 and caspase-1, core components of the inflammasome[17], were minimally expressed in RGCs of control mice. In contrast, TgAPPswePS1 mice exhibited strong red fluorescence signals for both proteins within the RGC layer. Quantitative analysis showed significant upregulation, with 1.589±0.450-fold and 1.403±0.317-fold increases in NLRP3 and caspase-1 expression, respectively, in transgenic mice compared to controls ($P<0.01$).

GSDMD, the terminal executor of pyroptosis[18], was also markedly elevated in the RGCs of TgAPPswePS1 mice, with

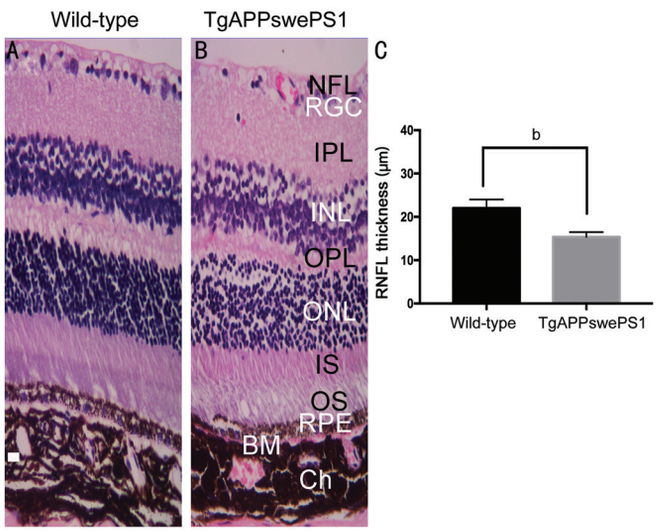

Figure 2 Histological evaluation of retinal morphology and RGC loss in wild-type and TgAPPswePS1 transgenic mice (scale bar=20 μm) A: H&E staining of the retina from a wild-type mouse; B: H&E staining of the retina from a TgAPPswePS1 transgenic mouse, revealing structural alterations; C: RNFL thickness is significantly decreased in TgAPPswePS1 mice relative to wild-type mice. $^{b}P<0.01$. H&E: Hematoxylin and eosin; RNFL: Retinal nerve fiber layer; RGC: Retinal ganglion cell layer; IPL: Inner plexiform layer; INL: Inner nuclear layer; OPL: Outer plexiform layer; ONL: Outer nuclear layer; IS: Inner segment; OS: Outer segment; RPE: Retinal pigment epithelium; BM: Bruch's membrane; Ch: Choroid.

intense immunoreactivity observed in the cytoplasm. The level of GSDMD expression was 4.735±1.071-fold higher in the experimental group than in controls ($P<0.01$), suggesting activation of the pyroptotic cascade.

Consistent with upstream inflammasome activation, downstream cytokines IL-1β[19] and IL-18[20]—hallmarks of pyroptosis-associated inflammation—were also significantly elevated. Immunofluorescence analysis revealed minimal expression in control retinas, while strong immunoreactivity was detected in RGCs of TgAPPswePS1 mice. Quantification showed 2.973±0.428-fold and 3.426±1.343-fold increases in IL-1β and IL-18 expression, respectively, in the transgenic group ($P<0.01$; Figure 3). These findings indicate that pyroptotic signaling is activated in RGCs of aged TgAPPswePS1 mice, potentially contributing to Aβ-mediated neuroinflammation and cell death.

DISCUSSION

RGCs is a defining feature of retinal degenerative diseases and a major contributor to vision impairment[21]. One of the pathological mechanisms implicated in this degeneration is Aβ accumulation, a process well-characterized in AD and increasingly recognized in retinal pathology[22]. In this study, we provide compelling evidence that Aβ deposition in the retina contributes to RGC structural damage and death in aged TgAPPswePS1 transgenic mice. More importantly, we identify pyroptosis—a form of inflammatory programmed cell death—as a potential mechanism underlying this Aβ-induced neurotoxicity.

Our first key finding is the prominent accumulation of APP and Aβ in the RGC layer of aged TgAPPswePS1 mice. Using APP- and Aβ-specific antibodies, we observed strong immunoreactivity localized within RGCs, consistent with previous reports indicating that RGCs may serve as a significant source of retinal Aβ[2,23]. This age-dependent amyloid burden is paralleled by a marked reduction in both RGC number and RNFL thickness, indicating that Aβ accumulation is not merely a passive event but likely contributes to neurodegeneration. These structural deficits align with prior observations in aged APP/PS1 models[24], reinforcing the relevance of this transgenic line for studying Aβ-related retinal degeneration.

The second major contribution of this study lies in the identification of pyroptosis as a potential pathway mediating RGC loss. We observed significant upregulation of pyroptosis-related markers, including NLRP3 inflammasome components, caspase-1, and cleaved GSDMD, in the retina of TgAPPswePS1 mice. These findings suggest that Aβ may trigger inflammasome activation and the subsequent cleavage of GSDMD, leading to pore formation in the plasma membrane and initiating pyroptotic cell death. This was further supported by the upregulation of the pro-inflammatory cytokines IL-1β and IL-18, which are canonical downstream products of caspase-1-mediated cleavage and key amplifiers of neuroinflammation[25]. These results collectively point to pyroptosis, rather than apoptosis alone, as a significant contributor to RGC death in this model.

Importantly, our findings build on and extend prior work demonstrating Aβ-induced activation of the NLRP3 inflammasome in the central nervous system[26-27]. While previous retinal studies have emphasized apoptosis, our data suggest that pyroptotic signaling may represent a previously underappreciated axis of RGC vulnerability, potentially driven by Aβ-induced oxidative stress and microglial activation[28-30]. This expands the current understanding of retinal neuroinflammation and opens the door to targeting pyroptosis as a therapeutic strategy in retinal degenerative diseases with amyloid pathology.

However, this study is not without limitations. The RNFL thickness measurements were conducted on postmortem tissue, which may not fully capture dynamic *in vivo* processes[31]. Moreover, although we observed elevated expression of pyroptosis-related proteins, we did not directly assess membrane pore formation or the characteristic cell swelling and lysis associated with pyroptosis. Additional *in vivo*

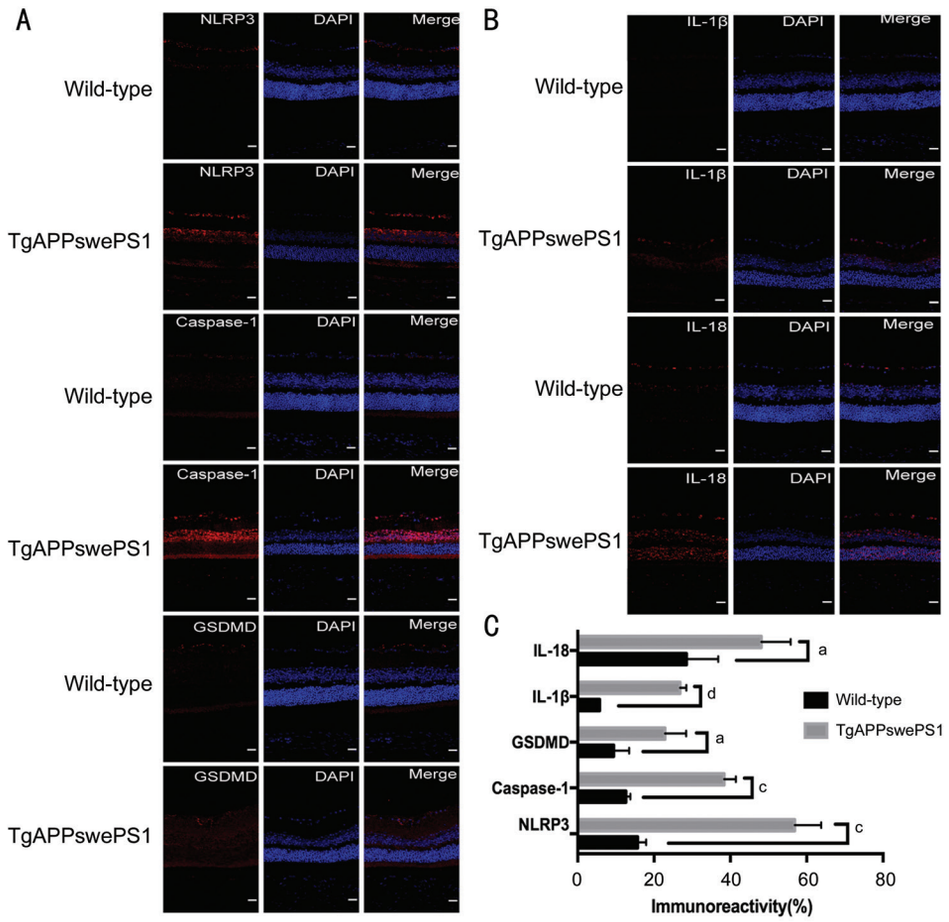

Figure 3 Immunofluorescence analysis of pyroptosis-related protein expression in RGCs of wild-type and TgAPPswePS1 transgenic mice (scale bar=20 μm) A: Representative images showing increased expression of NLRP3, caspase-1, and GSDMD in RGCs of TgAPPswePS1 mice; B: Elevated expression of inflammatory cytokines IL-1β and IL-18 in RGCs of TgAPPswePS1 mice; C: Semi-quantitative analysis of fluorescence intensity reveals significant upregulation of NLRP3, caspase-1, GSDMD, IL-1β, and IL-18 in TgAPPswePS1 mice compared to wild-type controls. $^{a}P<0.05$, $^{c}P<0.001$, $^{d}P<0.0001$. IL: Interleukin; RGC: Retinal ganglion cell layer; GSDMD: Gasdermin D; NLRP3: NOD-like receptor thermal protein domain associated protein 3; DAPI: 4',6-diamidino-2-phenylindole.

imaging and ultrastructural studies are needed to confirm pyroptotic morphology. Finally, while our data strongly associate Aβ with pyroptosis activation in RGCs, the molecular intermediates linking Aβ accumulation to inflammasome assembly and GSDMD cleavage remain to be elucidated. Further mechanistic studies are still needed to elucidate the relevant molecular mechanisms at the cellular level.

In conclusion, our study demonstrates that aged TgAPPswePS1 transgenic mice exhibit marked accumulation of APP and Aβ within RGCs, accompanied by significant structural degeneration, including reduced thinning of the nerve fiber layer. This pathological remodeling is closely associated with the activation of pyroptosis-related pathways, as evidenced by elevated expression of NLRP3, caspase-1, GSDMD, IL-1β, and IL-18 in RGCs. These findings suggest that Aβ deposition may trigger inflammatory cell death in RGCs through pyroptosis, thereby contributing to retinal neurodegeneration. By highlighting pyroptosis as a novel mechanism in Aβ-related retinal damage, this study expands the current understanding of retinal pathophysiology and points toward inflammasome signaling as a promising therapeutic target. Further research is needed to dissect the upstream molecular events linking Aβ to pyroptosis activation and to evaluate the therapeutic potential of pyroptosis inhibition in preserving retinal integrity and function.

ACKNOWLEDGEMENTS

Foundations: Supported by Natural Science Foundation of Zhejiang Province (No.LY18H120009); Wenzhou Basic Scientific Research Project (No.2025K0279); Xi'an Health and Wellness Committee General Cultivation Project (No.2023ms08); Shaanxi Province Health and Health High-Level Talents (Team) Training Program Young Talents Project.

Conflicts of Interest: Cao JR, None, **Li J,** None, **Zheng HH,** None, **Dong ZZ,** None.

REFERENCES

1 Morgia CL, di Vito L, Carelli V, *et al*. Patterns of retinal ganglion cell damage in neurodegenerative disorders: parvocellular vs magnocellular degeneration in optical coherence tomography studies. *Front Neurol* 2017;8:710.

2 Zhang Y, Chen HQ, Li R, *et al*. Amyloid β-based therapy for Alzheimer's disease: challenges, successes and future. *Sig Transduct Target Ther* 2023;8:248.

3 Reddy PH, Oliver DM. Amyloid beta and phosphorylated tau-induced defective autophagy and mitophagy in Alzheimer's disease. *Cells* 2019;8(5):488.

4 Murphy MP, LeVine H 3rd. Alzheimer's disease and the amyloid-beta peptide. *J Alzheimers Dis* 2010;19(1):311-323.

5 Wang L, Mao XB. Role of retinal amyloid-β in neurodegenerative diseases: overlapping mechanisms and emerging clinical applications. *Int J Mol Sci* 2021;22(5):2360.

6 Lazaldin MAM, Iezhitsa I, Agarwal R, *et al*. Neuroprotective effects of exogenous brain-derived neurotrophic factor on amyloid-beta 1-40-induced retinal degeneration. *Neural Regen Res* 2023;18(2):382-388.

7 Liu YF, Pan RJ, Ouyang YZ, *et al*. Pyroptosis in health and disease: mechanisms, regulation and clinical perspective. *Signal Transduct Target Ther* 2024;9(1):245.

8 Bergsbaken T, Fink SL, Cookson BT. Pyroptosis: host cell death and inflammation. *Nat Rev Microbiol* 2009;7(2):99-109.

9 Wang C, Yang T, Xiao JQ, *et al*. NLRP3 inflammasome activation triggers gasdermin D-independent inflammation. *Sci Immunol* 2021;6(64):eabj3859.

10 Kelley N, Jeltema D, Duan YH, *et al*. The NLRP3 inflammasome: an overview of mechanisms of activation and regulation. *Int J Mol Sci* 2019;20(13):3328.

11 Oladapo A, Jackson T, Menolascino J, *et al*. Role of pyroptosis in the pathogenesis of various neurological diseases. *Brain Behav Immun* 2024;117:428-446.

12 Cao J, Li J, Zheng H, *et al*. High-fat diet activates pyroptosis of retinal pigment epithelial cells in aged TgAPPswePS1 transgenic mice. *Eur J Med Res* 2025;30(1):635.

13 Lin RY, Hu CY, Shen TY, *et al*. Egr1/Gc/vitamin transport axis mediates synergistic effect of macular thinning and underweight in age-related visual acuity decline. *Exp Eye Res* 2025;258:110525.

14 Zhao AT, Nair RM, Lee EB, *et al*. Retinal imaging and tissue analysis for frontotemporal degeneration: recent advances and challenges for biomarker development. *J Neurol Neurosurg Psychiatry* 2025:jnnp-2024-335723.

15 Cui XX, Yi CJ, Liu J, *et al*. The gut microbial system responds to retinal injury and modulates the outcomes by regulating innate immune activation. *Invest Ophthalmol Vis Sci* 2025;66(9):6.

16 Chen GF, Xu TH, Yan Y, *et al*. Amyloid beta: structure, biology and structure-based therapeutic development. *Acta Pharmacol Sin* 2017;38(9):1205-1235.

17 Zhang WJ, Li KY, Lan Y, *et al*. NLRP3 inflammasome: a key contributor to the inflammation formation. *Food Chem Toxicol* 2023;174:113683.

18 He WT, Wan HQ, Hu LC, *et al*. Gasdermin D is an executor of pyroptosis and required for interleukin-1β secretion. *Cell Res* 2015;25(12):1285-1298.

19 Li Y, Jiang QZ. Uncoupled pyroptosis and IL-1β secretion downstream of inflammasome signaling. *Front Immunol* 2023;14:1128358.

20 Hou JW, Hsu JM, Hung MC. Molecular mechanisms and functions of pyroptosis in inflammation and antitumor immunity. *Mol Cell* 2021;81(22):4579-4590.

21 Lin B, Peng EB. Retinal ganglion cells are resistant to photoreceptor loss in retinal degeneration. *PLoS One* 2013;8(6):e68084.

22 Sadigh-Eteghad S, Sabermarouf B, Majdi A, *et al*. Amyloid-beta: a crucial factor in Alzheimer's disease. *Med Princ Pract* 2015;24(1):1-10.

23 Lee S, Jiang KL, McIlmoyle B, *et al*. Amyloid beta immunoreactivity in the retinal ganglion cell layer of the Alzheimer's eye. *Front Neurosci* 2020;14:758.

24 Chen H, Epelbaum S, Delatour B. Fiber tracts anomalies in APPxPS1 transgenic mice modeling Alzheimer's disease. *J Aging Res* 2011;2011:281274.

25 Exconde PM, Hernandez-Chavez C, Bourne CM, *et al*. The tetrapeptide sequence of IL-18 and IL-1β regulates their recruitment and activation by inflammatory caspases. *Cell Rep* 2023;42(12):113581.

26 Lučiūnaitė A, McManus RM, Jankunec M, *et al*. Soluble Aβ oligomers and protofibrils induce NLRP3 inflammasome activation in microglia. *J Neurochem* 2020;155(6):650-661.

27 Xu W, Huang Y, Zhou RB. NLRP3 inflammasome in neuroinflammation and central nervous system diseases. *Cell Mol Immunol* 2025;22(4):341-355.

28 Mou ZN, Zheng YF, Wang XC, *et al*. Vitamin C reduces the loss of retinal ganglion cells in chronic glaucoma by inhibiting neuroinflammation. *Nutr Neurosci* 2025:1-19.

29 Xu YY, Ye XT, Du YF, *et al*. Nose-to-brain delivery of targeted lipid nanoparticles as two-pronged β-amyloid nanoscavenger for Alzheimer's disease therapy. *Acta Pharm Sin B* 2025;15(6):2884-2899.

30 Ardura-Fabregat A, Bosch LFP, Wogram E, *et al*. Response of spatially defined microglia states with distinct chromatin accessibility in a mouse model of Alzheimer's disease. *Nat Neurosci* 2025;28(8):1688-1703.

31 Munguba GC, Galeb S, Liu Y, *et al*. Nerve fiber layer thinning lags retinal ganglion cell density following crush axonopathy. *Invest Ophthalmol Vis Sci* 2014;55(10):6505-6513.